Behavioural Brain Research 393 (2020) 112777

Contents lists available at ScienceDirect

Behavioural Brain Research

journal homepage: www.elsevier.com/locate/bbr

Cognitive impairments in adult mice with RIP140 overexpression in neural stem cells

Xinjuan Wang[a,1], Shimeng Ren[c,1], Weidong Yu[a], Qing Mu[a], Shuai Ye[c], Cailian Cui[b,*], Jingzhu Guo[c,*]

[a] Department of Central Laboratory & Institute of Clinical Molecular Biology, Peking University People's Hospital, Beijing 100044, China
[b] Department of Neurobiology, School of Basic Medical Sciences, Neuroscience Research Institute, Key Laboratory for Neuroscience of the Ministry of Education/National Health Commission, Peking University, Beijing 100191, China
[c] Department of Pediatric, Peking University People's Hospital, Beijing 100044, China

ARTICLE INFO

Keywords:
Receptor-interacting protein 140
Neural stem cells
Cognitive function
Subgranular zone
Sub ventricular zone

ABSTRACT

Receptor-interacting protein 140 (RIP140) is a transcription co-regulator of several transcription factors and a signal transduction regulator. RIP140 was recently implicated in the regulation of cognitive functions. The gene that encodes RIP140 is located on chromosome 21. An increase in RIP140 expression was observed in the fetal cerebral cortex and hippocampus in Down syndrome patients who exhibited strong cognitive disabilities. We hypothesized that RIP140 overexpression affects cognitive function in adult neural development. The present study used a Cre-dependent adeno-associated virus to selectively overexpress RIP140 in neural stem cells using nestin-Cre mice. RIP140 overexpression efficiency was evaluated at the subgranular zone (SGZ) of the dorsal dentate gyrus (dDG) and the subventricular zone (SVZ) of the lateral ventricles (LVs). Mice with RIP140 overexpression in the SGZ exhibited deficits in cognitive function and spatial learning and memory, measured in the Morris water maze, object-place recognition test, and novel object recognition test. However, overexpression of RIP140 in SVZ only impaired performance in the Morris water maze and novel object recognition test but not in the object-place recognition test. Altogether, these results indicated defects in cognitive functions that were associated with RIP140 overexpression in neural stem cells and revealed a behavioral phenotype that may be used as a framework for further investigating the neuropathogenesis of Down syndrome.

1. Introduction

RIP140, also referred to as nuclear receptor-interacting protein-1 (NRIP1), is recognized for its functional role as a wide-spectrum transcriptional co-regulator [1]. RIP140 was shown to be significantly upregulated in the fetal cerebral cortex in Down syndrome (DS) patients compared with non-DS controls in our previous study [2]. An increase in RIP140 protein expression was reported in the hippocampus in DS patients who exhibited strong cognitive disabilities [3]. The gene that encodes RIP140 is located on chromosome 21 [4]. DS, also known as trisomy 21, is the most commonly known disorder of intellectual disability that is associated with neurodevelopmental alterations and the overexpression of selected genes on chromosome 21 [5–7]. Therefore, the trisomy of chromosome 21 appears to be the root cause of DS, but understanding chromosome 21 genes that are associated with brain development and function in DS remains a challenge [8].

The role of RIP140 regulating brain development is not fully understood. Changes in RIP140 expression influence cognition. Our previous study found that RIP140 overexpression promoted the neuronal differentiation of Neuro-2a cells [9]. RIP140 expression was highly correlated with the differentiation of human embryonic stem cells [10]. Much evidences show that RIP140 is directly involved in cognitive plasticity *via* modulating the nuclear receptor transcriptional activities. For instance, hippocampal estrogen receptor and glucocorticoids, which interacted with RIP140, have been involved in learning and memory formation [11–14]. Thus, to extend previous research, we hypothesized that RIP140 overexpression would affect behavioral cognitive function during neural development.

To test this hypothesis, we overexpressed RIP140 selectively in neural stem cells (NSCs) in adult mice to better study the effect of RIP140 overexpression on neural development. In the mammalian brain, adult neurogenesis under normal conditions is confined to two

* Corresponding authors.
E-mail addresses: clcui@bjmu.edu.cn (C. Cui), jingzhu.guo@bjmu.edu.cn (J. Guo).
[1] These authors contributed equally to this work.

https://doi.org/10.1016/j.bbr.2020.112777
Received 16 December 2019; Received in revised form 27 May 2020; Accepted 16 June 2020
Available online 21 June 2020
0166-4328/

regions: SVZ, which lines the lateral wall of the LVs and SGZ in the hippocampal dentate gyrus [15]. These two regions receive and integrate newborn neurons throughout adult life. NSCs in these regions continuously generate new neurons that are functionally integrated into neural circuits [16]. The dysfunction of adult neurogenesis is closely related to brain disorders [17]. Knocking down neurogenesis has been found to result in specific cognitive deficits. Spatial memory was affected in many instances, in particular long-term memory retention in the Morris water maze test [18]. Context-dependent memory was also found to depend on neurogenesis [19,20]. Mice with increased neurogenesis, either through behavioral interventions (exercise, enriched environment) or by genetically enhancing the survival of new neurons, improved the ability to distinguish nearby locations on touchscreen task [21] or similar fear conditioning contexts [22,23].

We adopted a Cre-dependent adeno-associated virus (AAV) that was microinjected in the SVZ and SGZ to selectively overexpress RIP140 in nestin-Cre mice using a Cre-lox recombination system [24,25]. These mice were analyzed in the Morris water maze, object-place recognition test, and novel object recognition test to assess cognitive function, spatial learning and memory, and general activity. We uncovered a major role for RIP140 in the central nervous system in processes that are involved in cognitive function from a neurodevelopmental perspective.

2. Material and methods

2.1. Animals

Male C57BL/6 mice (6–8 weeks of age) were provided by the Department of Laboratory Animal Sciences, Peking University Health Science Center. CRE recombinase in B6.Cg-Tg (Nes-cre) 1Kln/J mice is driven by the endogenous nestin promoter [24]. Transgenic mice were bred on a C57BL/6 background. All animals received food and water *ad libitum*. The mice were housed five per cage with controlled temperature (23 °C ± 2 °C) and humidity (50 % ± 5%) under a 12 h/12 h light/dark cycle. All experimental procedures were approved by the Ethical Review Committee of Peking University People's Hospital and the Animal Use Committee of Peking University Health Science Center.

Polymerase chain reaction (PCR) genotyping was performed using genomic DNA that was extracted from the tip of the tail using a mouse genotyping kit (catalog no. AD501 − 02, Transgen Biotech, Beijing, China, Fig. 1B). The PCR primer sequences for CRE were the following: Forward (5′-ATTTGCCTGCATTACCGGTC-3′) and reverse (5′-ATCAAC GTTTTCTTTTCGG-3′) [24].

2.2. Adeno-associated virus

The Cre-dependent viral vector was packaged by inserting the mouse RIP140 coding sequence into a nEF1a-promoted rAAV2/9-DIO-Flag-WPREs vector (BrainVTA, Wuhan, China; Fig. 1A). Microinjection of the AAV-RIP140 in the LVs and dDG in nestin-Cre mice results in RIP140 overexpression in nestin-expressing neural progenitor cells. The viral vector without RIP140 gene insertion was used as a control.

For stereotaxic injections, the nestin-Cre mice were anesthetized with ketamine (100 mg/kg) and xylazine hydrochloride (10 mg/kg). rAAV-nEF1a-DIO-*RIP140*-Flag-pA (titer: 2.21E + 12 vg/mL) was bilaterally microinjected in the LVs (anterior/posterior, −0.6 mm; medial/lateral, ± 1.0 mm; dorsal/ventral, −2.0 mm; 1 μl/site, 0.1 μl/min) and dDG (anterior/posterior, -1.7 mm; medial/lateral, ± 1.0 mm; dorsal/ventral, −1.7 mm; 0.3 μl/site, 0.05 μl/min) of nestin-Cre mice. The control virus of rAAV-nEF1a-DIO-Flag-pA (titer: 3.24E + 12 vg/mL) was also bilaterally microinjected into the LVs and dDG of nestin-Cre mice. To allow the solution to diffuse into brain tissue, the needle was left in place for an additional 5 min after the injection. The stereotaxic coordinates were based on the Franklin and Paxinos *Mouse Brain in Stereotaxic Coordinates*, 3rd edition. After virus expression for 4 weeks, the mice were used in the subsequent experiments. The injection sites were histologically verified in all mice. Mice with off-target expression were excluded from further analysis.

2.3. Behavioral testing

After the virus expression for 4 weeks, behavioral tests started. The order of behavior test was object-place recognition test, novel object recognition test and finally Morris water maze. The interval between each behavior test was 24 h. Behavioral tests were performed during the light phase (9:00 A.M. to 3:00 P.M.).

2.3.1. Object-place recognition test

The mice were handled for 5 min and habituated in a 40 cm × 40 cm × 40 cm box that was marked with visual cues without objects for 30 min per day for 2 days before the test. The test consisted of two phases [26]. In the sample phase, the mice were placed in the box with two identical objects (two cubes, arbitrarily named O_A and O_B) at two different corners. The mice were allowed to explore freely for 2 min before they were removed from the box. The box and objects were cleaned with 75 % ethanol. Pseudorandomly, one of the two objects (O_A) remained unchanged and left in the same place, whereas the other object (O_B) was moved to a new corner. In the test phase, the mice were placed in the box again and allowed to explore for 2 min. When the mouse headed to and contacted the object with its nose, one exploration was counted. The bias score was calculated as exploration time:

$$(O_B - O_A) / (O_B + O_A).$$

2.3.2. Novel object recognition test

The protocol was similar to the object-place recognition test. However, during the removal period, one of the two objects (O_A) remained unchanged and was left in the same place, whereas the other object (O_B) was changed to a cylinder (O_C). The preference for the novel object was measured. The bias score for sample phase was calculated as exploration time: $(O_B - O_A) / (O_B + O_A)$. The bias score for test phase was calculated as exploration time:

$$(O_C - O_A) / (O_C + O_A).$$

2.3.3. Morris water maze

The maze consisted of a round pool (120 cm diameter) and round transparent plastic platform (10 cm diameter, placed in the center of the first quadrant, 1 cm below the water surface). The water was 50 cm deep (23 °C ± 2 °C). Patterns of different shapes and combinations were used as visual cues for the mice to locate the hidden platform. Milk was added to the water to facilitate tracking the swimming paths of the mice. The Morris water maze test was performed as previously described [27]. Briefly, we trained the mice in four trials per day with different starting points for 5 consecutive days. The intertrial interval was 10 min. The latency for each animal to find and remain on the platform for at least 3 s was recorded, and the cut-off time was set at 60 s. If an animal failed to find the platform within the allotted time, then it was placed on the platform for 15 s. On day 6, the platform was removed, and the mice were allowed to search freely for 1 min starting from the third quadrant. The number of entries into the platform area, total time spent in the first quadrant, and latency to reach the platform were recorded.

All behavioral parameters were measured using the ANY-maze video tracking system (version 4.99 m, Stoelting).

2.4. Immunostaining

The immunostaining assay was conducted as previously described [28]. The mice were anesthetized with 1% pentobarbital sodium and

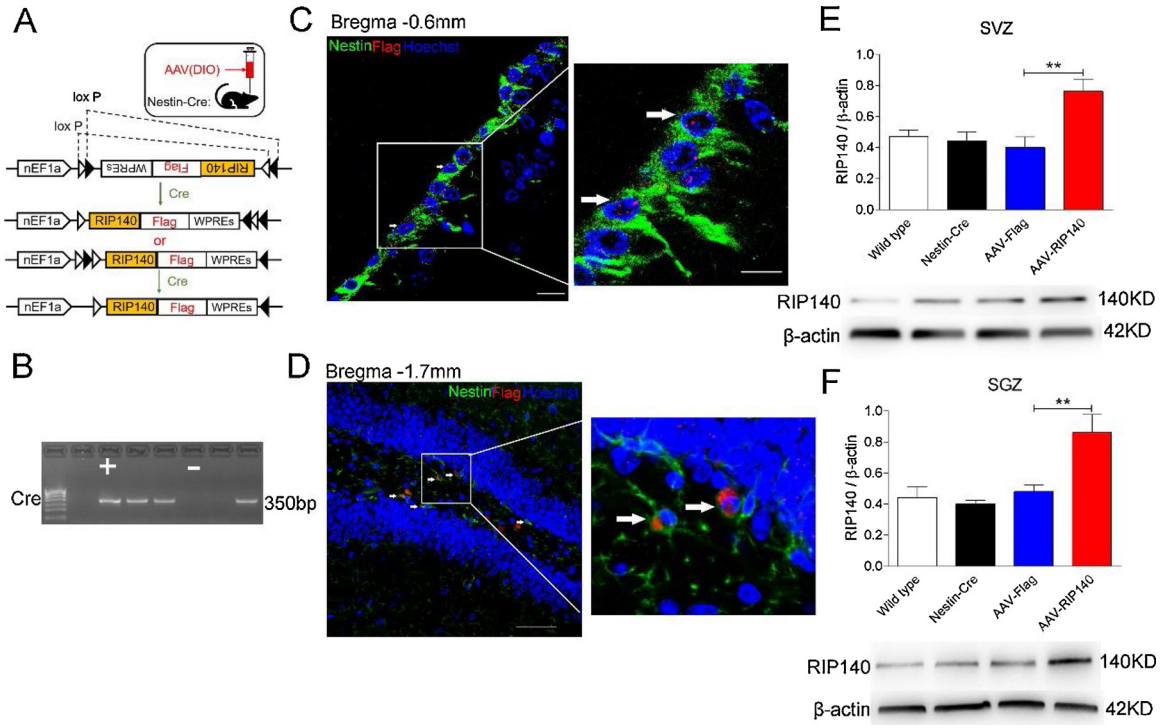

Fig. 1. Selective RIP140 overexpression in neural stem cells in the SVZ and SGZ by Cre-dependent viral vector. (A) Diagram that shows the strategy for conditional *RIP140* overexpression in neural stem cells in mice. AAV-Flag was used as the control virus. (B) Genotyping of nestin-Cre mice by PCR. +, nestin-Cre-positive mice; –, nestin-Cre-negative mice. Representative images of Flag, Nestin, and Hoechst labeling in the SVZ in the LVs (C) and SGZ of the dDG (D) 28 days after the AAV-RIP140 injection. (C) Magnified views (scale bar, 10 μm) of areas in the white box are shown in the right of the image. (D) Magnified views of areas in the white box are shown in the right of the image. Scale bar, 50 μm. Western blot that show RIP140 overexpression with AAV-RIP140 in the SVZ (E) and SGZ (F). $^{**}p < 0.01$, compared with AAV-Flag (one-way ANOVA followed by Bonferroni's *post hoc* test). n = 8/group.

intracardially perfused with 4% paraformaldehyde (PFA) in 0.1 M phosphate buffer, pH 7.4. The brains were postfixed with 4% PFA for 24 h and then consecutively transferred to 20 % and 30 % sucrose solutions. Three coronal brain sections (30 μm thick, LVs including anterior/posterior -0.5 mm, -0.6 mm, -0.7 mm; dDG including anterior/posterior -1.6 mm, -1.7 mm, -1.8 mm) were sliced in each mouse using a cryostat microtome (model 1950, Leica). Free-floating sections were washed in phosphate-buffered saline (PBS), blocked with buffer that contained 5% bovine serum albumin and 0.3 % Triton X-100 for 1 h, and incubated with the following primary antibodies at 4 ˚C for 24 h: mouse anti-Nestin (1:200, catalog no. ab6142, Abcam, Cambrige, UK) and rabbit anti-FLAG (1:500, catalog no. 14793, Cell Signaling Technology, Danvers, MA, USA). The sections were then washed in PBS and incubated with the following secondary antibodies at room temperature for 90 min. Alexa Fluor 488-conjugated donkey anti-mouse IgG (1:500, catalog no. A21202, Invitrogen, Carlsbad, CA, USA), Alexa Fluor 555-conjugated donkey anti-rabbit IgG (1:500, catalog no. A31572, Invitrogen, Carlsbad, CA, USA), and Hoechst33258 (1:500, catalog no. H3569, Invitrogen, Carlsbad, CA, USA). After rinsing extensively with PBS, the sections were transferred to slides and coverslipped using antifade solution (C1210, Applygen, Beijing, China). Images were taken using a laser-scanning confocal microscope (model FV1000, Olympus, Tokyo, Japan).

2.5. Western blot

After AAV expression for 4 weeks, the brains of the mice were removed and frozen in liquid nitrogen. Samples were stored at −80 ˚C until protein extraction. Bilateral LVs punches were obtained from 0.8 mm thick sections (anterior/posterior from -0.14 to -0.94 mm) taken on a sliding cryostat microtome using 12 gauge needle. Bilateral dDG punches were obtained from 1 mm thick sections (anterior/posterior from -1.3 to -2.3 mm). Tissues from the bilateral LVs and dDG were isolated with RIPA buffer (R0278, Sigma Aldrich, St. LOUIS, MO, USA). Protein content was determined using the BCA assay (catalog no. 23225, Millipore, Billerica, MA, USA). Western blot was performed as previously described [29]. Total protein (50 μg) was separated in sodium dodecyl sulfate-polyacrylamide gel electrophoresis (SDS-PAGE) gels and transferred to polyvinylidene difluoride (PVDF) membranes (ISEQ00010, Millipore, Billerica, MA, USA). The blots were blocked in TBST (TBS with 0.1 % Tween-20) that contained 5% nonfat milk for 1 h at room temperature and then incubated with the following primary antibodies that were diluted in TBST with 5% nonfat milk overnight at 4 ˚C with gentle shaking: mouse anti-β-actin (1:3000, catalog no. A2228, Sigma Aldrich, St. LOUIS, MO, USA) and rabbit anti-RIP140 (1:1000, catalog no. ab42126, Abcam, Cambridge, UK). The blots were then washed with TBST and incubated with horseradish peroxidase-conjugated goat anti-mouse IgG (1:2000, catalog no. ZB-2305, Zhongshan Biotechnology, Beijing, China) or goat anti-rabbit IgG (1:2000, catalog no. ZB-2301, Zhongshan Biotechnology, Beijing, China) for 1 h at room temperature. Protein blots were detected using a chemiluminescence detection kit (WBKLS0500, Millipore, Billerica, MA, USA) and quantitatively analyzed by densitometry using ImageJ software. Relative expression was normalized to β-actin protein expression.

2.6. Statistical analysis

The statistical analysis was performed using GraphPad Prism 6.0 software. Comparisons between groups were performed using one-way analysis of variance (ANOVA) followed by Bonferroni's *post hoc* test, or two-way ANOVA followed by Tukey's *post hoc* test. Values of $p < 0.05$ were considered statistically significant. The data are presented as mean ± SEM.

3. Results

3.1. RIP140 was selectively overexpressed in neural stem cells in the SVZ and SGZ with Cre-dependent viral vector

To directly test whether RIP140 overexpression contributes to cognitive function in neural development, we adopted a Cre-dependent AAV to selectively overexpress RIP140 in neural stem cells in nestin-Cre mice using the Cre-Lox recombination system (Fig. 1A). In all of the experiments, transgenic mice were genotyped by PCR, and positive nestin-Cre mice were used (Fig. 1B). We microinjected the AAV (DIO) into the LVs and dDG. Virus infection was verified by colabeled Flag (AAV-RIP140 marker) and Nestin (neural progenitor cell marker) within the SVZ of the LVs (Fig. 1C) and SGZ of the dDG (Fig. 1D) 4 weeks after the AAV-RIP140 injection. Significant elevations of RIP140 levels were detected 4 weeks after the virus injection in the SVZ ($F_{3,28}$ = 6.968, p = 0.0012; Fig.1E) and SGZ ($F_{3,28}$ = 8.676, p = 0.0003; Fig. 1F). The results demonstrated the effectiveness of RIP140 overexpression by AAV-RIP140 in neural stem cells in the SVZ and SGZ.

3.2. RIP140 overexpression in adult neural stem cells in the SVZ and SGZ impaired spatial learning and memory

We next examined the way in which RIP140 overexpression modulated spatial learning and memory. Four weeks after the AAV-RIP140 injection in the SVZ, the mice underwent Morris water maze training and testing (Fig. 2A). An increase in the escape latency (Time: $F_{4,36}$ = 95.60, $p < 0.0001$; RIP140: $F_{3,27}$ = 25.67, $p < 0.0001$; Time × RIP140 interaction: $F_{12,108}$ = 1.778, p = 0.0608; Fig. 2B), an increase in the latency to first enter the platform zone ($F_{3,38}$ = 2.934, p = 0.0456; Fig. 2D), a decrease in the number of entries into the platform zone ($F_{3,38}$ = 5.609, p = 0.0028; Fig. 2E), and a decrease in the time spent in the target quadrant ($F_{3,38}$ = 11.54, $p < 0.0001$; Fig. 2F) were observed in RIP140-overexpressing mice compared with the AAV-Flag group. Representative swimming tracks for platform crossings during the test day are shown in Fig. 2C. No significant differences in swimming speed were observed ($F_{3,38}$ = 0.6004, p = 0.6187; Fig. 2G), indicating no effect on general activity. Thus, spatial learning and memory were significantly impaired by RIP140 overexpression in adult neural stem cells in the SVZ.

Similar to the SVZ, RIP140 overexpression in adult neural stem cells in the SGZ resulted in an increase in escape latency (Time: $F_{4,36}$ = 20.93, $p < 0.0001$; RIP140: $F_{2,18}$ = 8.523, p = 0.0025; Time × RIP140 interaction: $F_{8,72}$ = 0.2397, p = 0.9819; Fig. 3B), an increase in the latency to first enter the platform zone ($F_{2,32}$ = 5.421, p = 0.0094; Fig. 3D), a decrease in the number of entries into the platform zone ($F_{2,32}$ = 4.497, p = 0.0190; Fig. 3E), and a decrease in the time spent in the target quadrant ($F_{2,32}$ = 4.820, p = 0.0148; Fig. 3F), with no effect on swimming speed ($F_{2,32}$ = 0.5677, p = 0.5724; Fig. 3G) compared with the AAV-Flag group. Representative swimming tracks for platform crossings during the test day are shown in Fig. 3C. These results indicated that RIP140 overexpression in adult neural stem cells in the SVZ and SGZ impaired spatial learning and memory in mice, without affecting their baseline exploratory behaviors.

3.3. RIP140 overexpression in adult neural stem cells in the SVZ and SGZ impaired cognitive function

We also evaluated the effect of RIP140 overexpression on cognitive function in the object-place recognition test (Fig. 4A) and novel object recognition test (Fig. 4B). RIP140 overexpression in adult neural stem cells in the SVZ had little effect on object-place recognition ($F_{3,40}$ = 0.1451, p = 0.9322; Fig. 4C). However, we observed impairments in novel object recognition in mice with RIP140 overexpression, reflected by a decrease in bias scores toward novel objects in the test phase ($F_{3,40}$ = 4.820, p = 0.0059; Fig. 4D). Representative exploratory tracks in the test phase in the AAV-Flag and AAV-RIP140 groups are shown in Fig. 4C and D. Thus, these results indicated that RIP140 overexpression in adult neural stem cells in the SVZ impaired cognitive function in part.

RIP140 overexpression in the SGZ clearly impaired cognitive function, reflected by no preference for the moved objects in the test phase ($F_{2,33}$ = 4.236, p = 0.0230; Fig. 4E) and no preference for the novel objects in the test phase ($F_{2,33}$ = 4.653, p = 0.0166; Fig. 4F). Representative exploratory tracks in the test phase in the AAV-Flag and AAV-RIP140 groups are shown in Fig. 4E and F.

Altogether, these results paralleled the aforementioned findings on spatial learning and memory and indicated that RIP140 overexpression in adult neural stem cells in the SVZ and SGZ impaired cognitive function.

4. Discussion

Research methods that investigate the role of cell-type specificity in specific brain regions in behavioral cognitive function will be more precise for the study of complex behaviors. The present study explored the effects of RIP140 overexpression in neural stem cells on behavioral phenotypes in mice and identified impairments in cognitive function and spatial learning and memory that were associated with region-specific, system-selective alterations of intercellular crosstalk that modulates neural development. Our work demonstrated that RIP140 overexpression in neural stem cells in the SGZ and SVZ contributed to cognitive impairments.

RIP140 is expressed in the mouse brain, particularly in neurons in the cortex, hippocampus, and pituitary gland [30]. RIP140 levels also appear to be highly expressed during stages of neurodevelopment and reduced during aging [31,32]. Previous studies have shown that RIP140 is involved in Alzheimer's disease and neurological cognitive decline [33,34]. These findings were confirmed in the present study. One different finding was that RIP140 knockout ($RIP140^{-/-}$) mice exhibited marked memory impairments compared with wildtype controls [30], which is inconsistent with our conclusion. However, RIP140 knockout mice were reported to be approximately 15–20 % smaller than wildtype mice and presented with strong physiological deregulations, such as female infertility and alteration of metabolism in muscle [35,36]. Muscular weakness in RIP140 knockout mice performed lower general activity impacting the behavioral tests. These knockout mice express the whole-body inactivation of RIP140 gene expression, with no brain zone or cell type specificity. In contrast, we manipulated the RIP140 gene selectively in neural stem cells in the SVZ and SGZ with no other negative effects. In summary, it is obvious that different gene manipulation methods will have different effects on the physical state and behavior of mice, and thus produce different experimental results. Therefore, our conclusion does not conflict with theirs.

Neurogenesis has been behaviorally and biochemically linked to cognitive dysfunction [37]. Reduced neurogenesis is considered among the major neurodevelopmental defects leading to cognitive disability in DS [38]. Results obtained using brains of individuals with DS, DS-derived induced pluripotent stem cells (iPSCs), and neural progenitor cells (NPCs) from the hippocampus of DS mouse models as experimental systems, showed a decline in proliferation potency which occurred concurrently with alterations to neurogenesis in DS [39,40]. Neurogenesis is observed well into the postnatal period and throughout adulthood, primarily in two discrete brain regions: the SGZ of the DG and SVZ of the LVs [37]. Progenitors in the SGZ mature locally into granule neurons in the DG, sending axonal projections to the CA3 area and dendritic arbors in the molecular layer [41]. There is now sufficient evidence suggesting that adult hippocampal neurogenesis plays a crucial role in the spatial discrimination and pattern separation functions of the DG [42]. For example, the acquisition of spatial memory in the water maze is correlated with the proliferation and survival of newborn DG neurons [43]. Therefore, RIP140 overexpression in the SGZ

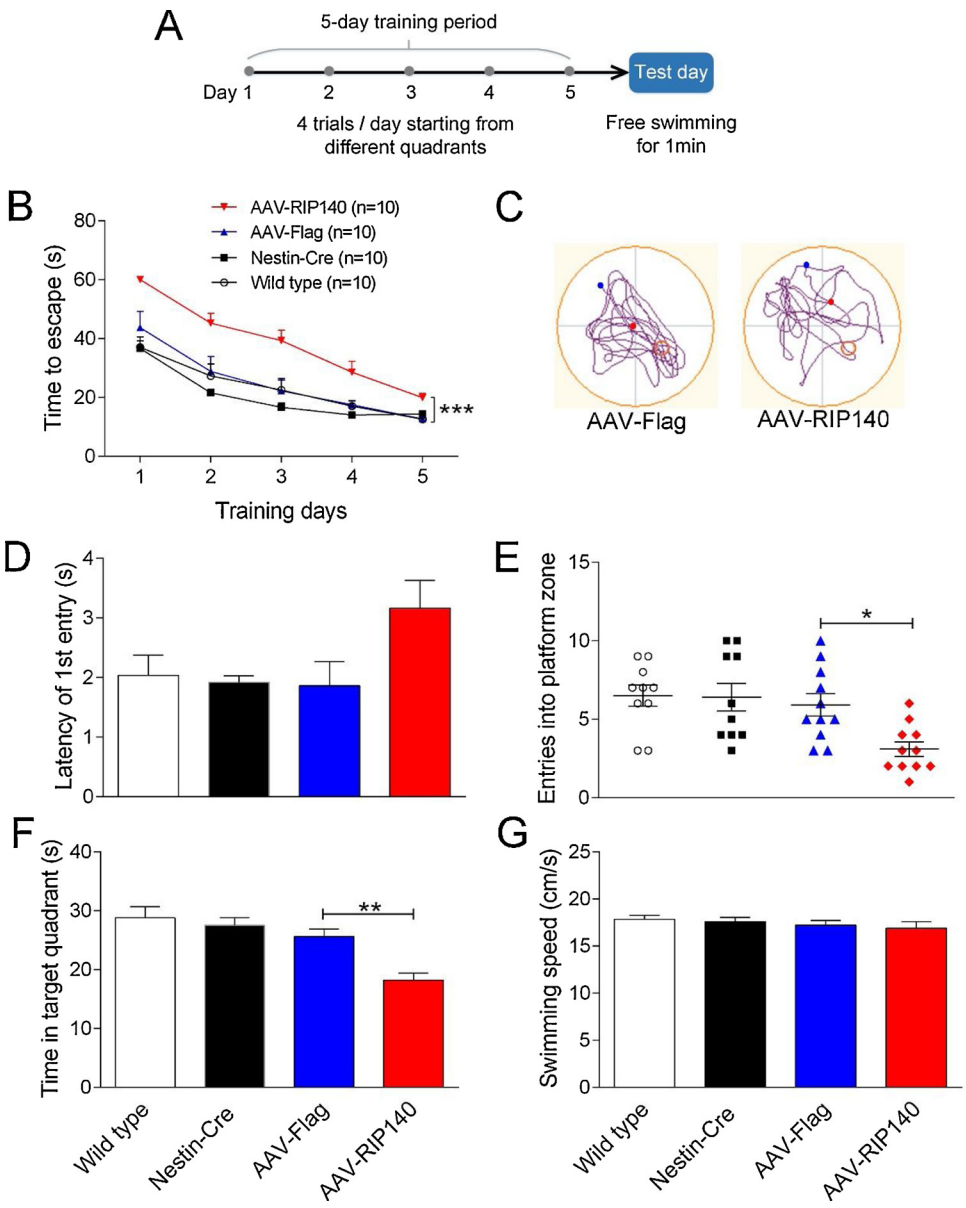

Fig. 2. RIP140 overexpression in adult neural stem cells in the SVZ impaired spatial learning and memory in mice. (A) Schematic diagram that shows the Morris water maze procedure. (B) Escape latency in mice in the training trials. The AAV-RIP140 group exhibited a longer escape latency during water maze training. ***$p < 0.001$, compared with AAV-Flag (two-way repeated-measures ANOVA followed by Tukey's *post hoc* test). (C) Representative swimming tracks for platform crossings during the test day. Blue dots indicate the starting position. Red dots indicate the ending position. Small circles indicate the platform position during training. (D) Latencies to enter the platform zone increased ($p = 0.084$, AAV-RIP140 *vs.* AAV-Flag) in the AAV-RIP140 group. (E) Total entries into the platform zone and (F) total time spent in the target quadrant decreased in the AAV-RIP140 group. (G) Swimming speed was unaffected on the test day. *$p < 0.05$, **$p < 0.01$, AAV-RIP140 *vs.* AAV-Flag (one-way ANOVA followed by Bonferroni's *post hoc* test for (D)-(G)).

impaired spatial memory and cognitive function (Figs. 3 and 4 E and F) in the Morris water maze, object-place recognition test, and novel object recognition test, which indicates RIP140 overexpression possibly disturbs neural neurogenesis in SGZ.

Animals in the SGZ in the novel object and object-place test had a natural preference for object A. This conclusion can be obtained from that bias score was negative value in the sample phase. When object B was moved or changed to object C, the number of explorations for object B or C increased in wild type group and AAV-Flag group. Therefore, bias score in the test phase tended to zero in this two groups. It indicated that mice in the wild type group and AAV-Flag group had the ability to explore changes in positions and novel objects. However, bias score is still negative value in the test phase for RIP140 overexpression group, indicating that behavioral exploration function was impaired and no preference for the moved objects and novel objects. Animals had a natural preference for object A, which did not affect our conclusion that RIP140 overexpression in the SGZ impaired cognitive exploration function.

However, RIP140 overexpression in the SVZ partially affected cognitive function with no effect on object-place recognition behavior test (Fig. 4C). Adult neurogenesis in the SVZ is known to contribute to perceptual and memory function, especially for olfactory memory, that is modulated by the olfactory bulb, in which newborn neurons in the SVZ migrate to the olfactory bulb or striatum and differentiate mostly into interneurons [44–46]. Recently, adult neurogenesis in the SVZ is increasingly recognized as a potential player in the development of psychiatric and cognitive disorders [47,48]. Thus, that RIP140 overexpression in the SVZ did not fully impair cognitive function, which is associated with visual cue memory rather than olfactory cue memory, is reasonable.

The present study assessed the behavioral effects of RIP140 overexpression selectively in neural stem cells and demonstrated that RIP140 overexpression in the SVZ and SGZ impaired cognitive processes. Unfortunately, the underlying mechanisms remain poorly understood. RIP140 regulates the transcriptional activity of several nuclear receptors, such as retinoid receptors, which are linked to memory processes [49,50]. RIP140 is responsible for decreased respiratory efficiency and altered morphology of mitochondria in DS [51,52]. RIP140 activity on mitochondrial pathways is mainly exerted through the repressive control on the transcriptional coactivator PGC-1α [53]. After *RIP140* silencing, the expression levels of *PGC-1α* and consequently the mitochondrial function are restored [51]. It is possibly that impairment

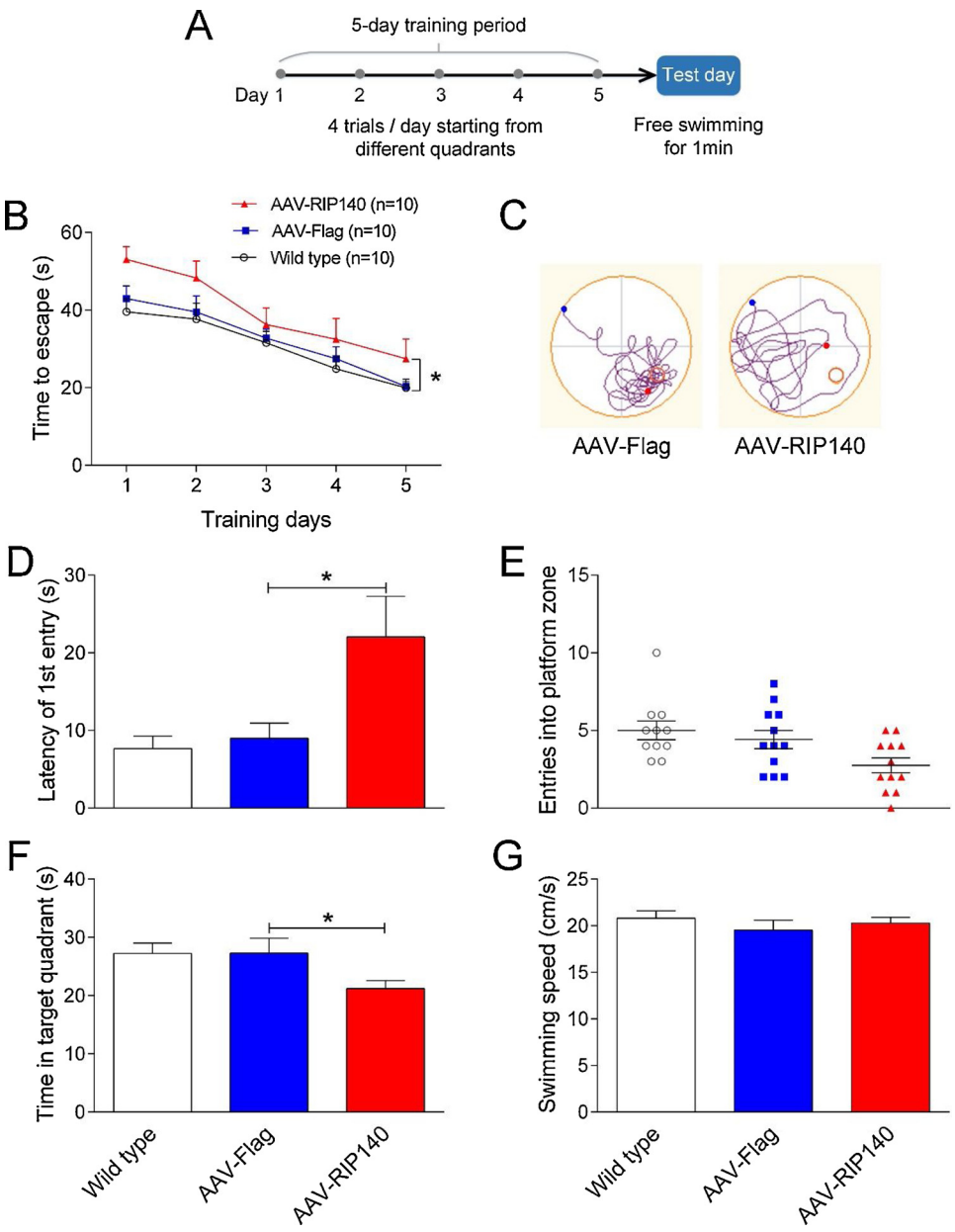

Fig. 3. RIP140 overexpression in adult neural stem cells in the SGZ impaired spatial learning and memory in mice. (A) Schematic diagram that shows the Morris water maze procedure. (B) Escape latency in mice in the training trials. The AAV-RIP140 group exhibited a longer escape latency during water maze training. *$p < 0.05$, compared with AAV-Flag (two-way repeated-measures ANOVA followed by Tukey's *post hoc* test). (C) Representative swimming tracks for platform crossings during the test day. Blue dots indicate the starting position. Red dots indicate the ending position. Small circles indicate the platform position during training. (D) Latencies to enter the platform zone increased in the AAV-RIP140 group. (E) Total entries into the platform zone ($p = 0.112$, AAV-RIP140 *vs.* AAV-Flag) and (F) total time spent in the target quadrant decreased in the AAV-RIP140 group. (G) Swimming speed was unaffected on the test day. *$p < 0.05$, AAV-RIP140 *vs.* AAV-Flag (one-way ANOVA followed by Bonferroni's *post hoc* test for (D)-(G)).

in signaling pathways controlling mitochondrial functions induces a reduction in mitochondrial ATP production and impairment in many ATP-dependent neurological process including neurogenesis [38]. Future studies should seek to confirm this possibility to provide comprehensive insights into the molecular mechanisms by which RIP140 contributes to cognitive function.

Overall, the present results confirmed a role for RIP140 overexpression in neural stem cells in cognitive function, which may help elucidate the pathogenesis of some neurological conditions, such as DS.

Authors contribution

Jingzhu Guo, Cailian Cui and Xinjuan Wang conceived and designed the research; Xinjuan Wang and Shimeng Ren performed all experiments, Xinjuan Wang drafted the manuscript; Weidong Yu, Qing Mu, Shuai Ye provided technical support; Jingzhu Guo and Xinjuan Wang edited and revised the manuscript.

CRediT authorship contribution statement

Xinjuan Wang: Conceptualization, Methodology, Investigation, Formal analysis, Writing - original draft, Writing - review & editing. **Shimeng Ren:** Methodology, Investigation, Formal analysis. **Weidong Yu:** Validation. **Qing Mu:** Validation. **Shuai Ye:** Validation. **Cailian Cui:** Conceptualization, Supervision. **Jingzhu Guo:** Conceptualization, Project administration, Writing - review & editing.

Declaration of Competing Interest

The authors declare no conflict of interest.

Acknowledgements

The work was supported by the National Natural Science Foundation of China (grant no. 31671066 and no. 81801348) and Peking University People's Hospital Scientific Research Development Funds (grant no. RDY2018-30). Sponsors do not participate in study

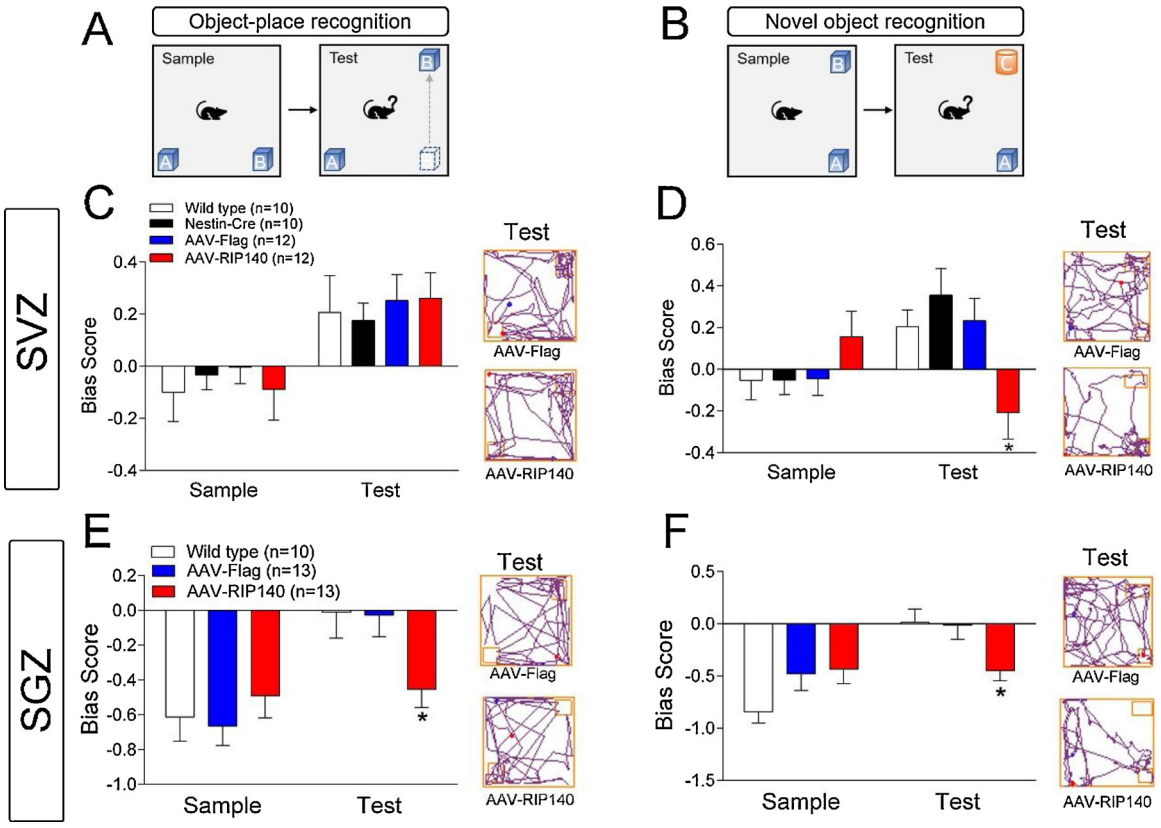

Fig. 4. RIP140 overexpression in adult neural stem cells in the SVZ and SGZ impaired cognitive ability in mice. Schematic diagram that shows the object-place recognition procedure (A) and novel object recognition procedure (B). (C, D) RIP140 overexpression in the SVZ had no effect on object-place recognition (C) but impaired novel object recognition (D). *$p < 0.05$, AAV-RIP140 *vs.* AAV-Flag (one-way ANOVA followed by Bonferroni's *post hoc* test). (E, F) RIP140 overexpression in the SGZ impaired object-place recognition (E) and novel object recognition (F). *$p < 0.05$, AAV-RIP140 *vs.* AAV-Flag (one-way ANOVA followed by Bonferroni's *post hoc* test). (C–F) Representative exploratory tracks (right) in the test phase in the AAV-Flag and AAV-RIP140 groups. (C, E) The square in the upper right corner indicates O_B. The square in the lower left corner indicates O_A. (D, F) The square indicates O_A, and the rectangle indicates O_C.

design, collection, data analysis, writing and manuscript submission. The authors thank the research group of professor You Wan for providing the B6.Cg-Tg (Nes-cre) 1Kln/J mice at Peking University Health Science Center.

References

[1] L.N. Wei, Retinoid receptors and their coregulators, Annu. Rev. Pharmacol. 43 (2003) 47–72.
[2] W.D. Yu, R. Liang, L.J. Yang, M. Shang, H. Shen, J. Guan, J.Z. Guo, Screening and identification of human chromosome 21 genes resulting in abnormal development of fetal cerebral cortex with Down syndrome, Natl. Med. J. China (in Chinese) 87 (39) (2007) 2759–2763.
[3] K. Gardiner, Transcriptional dysregulation in Down syndrome: predictions for altered protein complex stoichiometries and post-translational modifications, and consequences for learning/behavior genes ELK, CREB, and the estrogen and glucocorticoid receptors, Behav. Genet. 36 (3) (2006) 439–453.
[4] N. Katsanis, J.H. Ives, J. Groet, D. Nizetic, E.M. Fisher, Localisation of receptor interacting protein 140 (RIP140) within 100 kb of D21S13 on 21q11, a gene-poor region of the human genome, Hum. Genet. 102 (2) (1998) 221–223.
[5] S.E. Antonarakis, Down syndrome and the complexity of genome dosage imbalance, Nat. Rev. Genet. 18 (3) (2017) 147–163.
[6] T.F. Haydar, R.H. Reeves, Trisomy 21 and early brain development, Trends Neurosci. 35 (2) (2012) 81–91.
[7] K.B. Larsen, H. Laursen, N. Graem, G.B. Samuelsen, N. Bogdanovic, B. Pakkenberg, Reduced cell number in the neocortical part of the human fetal brain in Down syndrome, Ann. Anat. 190 (5) (2008) 421–427.
[8] J.L. Olmos-Serrano, H.J. Kang, W.A. Tyler, J.C. Silbereis, F. Cheng, Y. Zhu, M. Pletikos, L. Jankovic-Rapan, N.P. Cramer, Z. Galdzicki, J. Goodliffe, A. Peters, C. Sethares, I. Delalle, J.A. Golden, T.F. Haydar, N. Sestan, Down syndrome developmental brain transcriptome reveals defective oligodendrocyte differentiation and myelination, Neuron 89 (6) (2016) 1208–1222.
[9] X. Feng, W. Yu, R. Liang, C. Shi, Z. Zhao, J. Guo, Receptor-interacting protein 140 overexpression promotes neuro-2a neuronal differentiation by ERK1/2 signaling, Chin. Med. J. (Engl.) 128 (1) (2015) 119–124.
[10] Z.R. Zhao, W.D. Yu, C. Shi, R. Liang, X. Chen, X. Feng, X. Zhang, Q. Mu, H. Shen, J.Z. Guo, Correlation between receptor-interacting protein 140 expression and directed differentiation of human embryonic stem cells into neural stem cells, Neural Regen. Res. 12 (1) (2017) 118.
[11] H.N. Fugger, T.C. Foster, J. Gustafsson, E.F. Rissman, Novel effects of estradiol and estrogen receptor alpha and beta on cognitive function, Brain Res. 883 (2) (2000) 258–264.
[12] B.J. Kolber, L. Wieczorek, L.J. Muglia, Hypothalamic-pituitary-adrenal axis dysregulation and behavioral analysis of mouse mutants with altered glucocorticoid or mineralocorticoid receptor function, Stress 11 (5) (2008) 321–338.
[13] B. Roozendaal, Curt P. Richter award. Glucocorticoids and the regulation of memory consolidation, Psychoneuroendocrinology 25 (3) (1999) 213–238 2000.
[14] G. Sanchez-Andrade, K.M. Kendrick, Roles of alpha- and beta-estrogen receptors in mouse social recognition memory: effects of gender and the estrous cycle, Horm. Behav. 59 (1) (2011) 114–122.
[15] P.M. Lledo, M. Alonso, M.S. Grubb, Adult neurogenesis and functional plasticity in neuronal circuits, Nat. Rev. Neurosci. 7 (3) (2006) 179–193.
[16] E. Pastrana, L.C. Cheng, F. Doetsch, Simultaneous prospective purification of adult subventricular zone neural stem cells and their progeny, Procl. Natl. Acad. Sci. U. S. A. 106 (15) (2009) 6387–6392.
[17] K.M. Christian, H. Song, G.L. Ming, Functions and dysfunctions of adult hippocampal neurogenesis, Annu. Rev. Neurosci. 37 (2014) 243–262.
[18] J.T. Goncalves, S.T. Schafer, F.H. Gage, Adult neurogenesis in the Hippocampus: from stem cells to behavior, Cell 167 (4) (2016) 897–914.
[19] H.G. Ko, D.J. Jang, J. Son, C. Kwak, J.H. Choi, Y.H. Ji, Y.S. Lee, H. Son, B.K. Kaang, Effect of ablated hippocampal neurogenesis on the formation and extinction of contextual fear memory, Mol. Brain 2 (2009) 1.
[20] M.D. Saxe, F. Battaglia, J.W. Wang, G. Malleret, D.J. David, J.E. Monckton, A.D. Garcia, M.V. Sofroniew, E.R. Kandel, L. Santarelli, R. Hen, M.R. Drew, Ablation of hippocampal neurogenesis impairs contextual fear conditioning and synaptic plasticity in the dentate gyrus, Proc. Natl. Acad. Sci. U. S. A. 103 (46) (2006) 17501–17506.
[21] D.J. Creer, C. Romberg, L.M. Saksida, H. van Praag, T.J. Bussey, Running enhances spatial pattern separation in mice, Proc. Natl. Acad. Sci. U. S. A. 107 (5) (2010) 2367–2372.
[22] A. Sahay, K.N. Scobie, A.S. Hill, C.M. O'Carroll, M.A. Kheirbek, N.S. Burghardt, A.A. Fenton, A. Dranovsky, R. Hen, Increasing adult hippocampal neurogenesis is sufficient to improve pattern separation, Nature 472 (7344) (2011) 466–470.
[23] T. Toda, S.L. Parylak, S.B. Linker, F.H. Gage, The role of adult hippocampal

neurogenesis in brain health and disease, Mol. Psychiatry 24 (1) (2019) 67–87.
[24] J. Zheng, Y.Y. Jiang, L.C. Xu, L.Y. Ma, F.Y. Liu, S. Cui, J. Cai, F.F. Liao, Y. Wan, M. Yi, Adult hippocampal neurogenesis along the dorsoventral Axis Contributes differentially to environmental enrichment combined with voluntary exercise in alleviating chronic inflammatory pain in mice, J. Neurosci. 37 (15) (2017) 4145–4157.
[25] A. Soumier, E. Sibille, Opposing effects of acute versus chronic blockade of frontal cortex somatostatin-positive inhibitory neurons on behavioral emotionality in mice, Neuropsychopharmacol 39 (9) (2014) 2252–2262.
[26] P.D. Whissell, S. Rosenzweig, I. Lecker, D.S. Wang, J.M. Wojtowicz, B.A. Orser, Gamma-aminobutyric acid type A receptors that contain the delta subunit promote memory and neurogenesis in the dentate gyrus, Ann. Neurol. 74 (4) (2013) 611–621.
[27] C.V. Vorhees, M.T. Williams, Morris water maze: procedures for assessing spatial and related forms of learning and memory, Nat. Protoc. 1 (2) (2006) 848–858.
[28] N. Wang, F. Ge, C. Cui, Y. Li, X. Sun, L. Sun, X. Wang, S. Liu, H. Zhang, Y. Liu, M. Jia, M. Yang, Role of glutamatergic projections from the ventral CA1 to infralimbic cortex in context-induced reinstatement of heroin seeking, Neuropsychopharmacol 43 (6) (2018) 1373–1384.
[29] X. Wang, Y. Liu, M. Jia, X. Sun, N. Wang, Y. Li, C. Cui, Phosphorylated SNAP25 in the CA1 regulates morphine-associated contextual memory retrieval via increasing GluN2B-NMDAR surface localization, Addict. Biol. (2017).
[30] F. Duclot, M. Lapierre, S. Fritsch, R. White, M.G. Parker, T. Maurice, V. Cavailles, Cognitive impairments in adult mice with constitutive inactivation of RIP140 gene expression, Genes Brain Behav. 11 (1) (2012) 69–78.
[31] S. Ghosh, M.K. Thakur, Tissue-specific expression of receptor-interacting protein in aging mouse, Age Dordr. (Dordr) 30 (4) (2008) 237–243.
[32] L. Katsouri, K. Blondrath, M. Sastre, Peroxisome proliferator-activated receptor-gamma cofactors in neurodegeneration, IUBMB Life 64 (12) (2012) 958–964.
[33] S. Flaisher-Grinberg, H.C. Tsai, X. Feng, L.N. Wei, Emotional regulatory function of receptor interacting protein 140 revealed in the ventromedial hypothalamus, Brain Behav. Immun. 40 (2014) 226–234.
[34] K. Blondrath, J.H. Steel, L. Katsouri, M. Ries, M.G. Parker, M. Christian, M. Sastre, The nuclear cofactor receptor interacting protein-140 (RIP140) regulates the expression of genes involved in Abeta generation, Neurobiol. Aging 47 (2016) 180–191.
[35] R. White, G. Leonardsson, I. Rosewell, M. Ann Jacobs, S. Milligan, M. Parker, The nuclear receptor co-repressor nrip1 (RIP140) is essential for female fertility, Nat. Med. 6 (12) (2000) 1368–1374.
[36] A. Seth, J.H. Steel, D. Nichol, V. Pocock, M.K. Kumaran, A. Fritah, M. Mobberley, T.A. Ryder, A. Rowlerson, J. Scott, M. Poutanen, R. White, M. Parker, The transcriptional corepressor RIP140 regulates oxidative metabolism in skeletal muscle, Cell Metab. 6 (3) (2007) 236–245.
[37] D.M. Apple, R.S. Fonseca, E. Kokovay, The role of adult neurogenesis in psychiatric and cognitive disorders, Brain Res. 1655 (2017) 270–276.
[38] R.A. Vacca, S. Bawari, D. Valenti, D. Tewari, S.F. Nabavi, S. Shirooie, A.N. Sah, M. Volpicella, N. Braidy, S.M. Nabavi, Down syndrome: neurobiological alterations and therapeutic targets, Neurosci. Biobehav. Rev. 98 (2019) 234–255.
[39] A. Gimeno, J.L. Garcia-Gimenez, L. Audi, N. Toran, P. Andaluz, F. Dasi, J. Vina, F.V. Pallardo, Decreased cell proliferation and higher oxidative stress in fibroblasts from Down Syndrome fetuses. Preliminary study, Biochim. Biophys. Acta 1842 (1) (2014) 116–125.
[40] Y. Hibaoui, I. Grad, A. Letourneau, M.R. Sailani, S. Dahoun, F.A. Santoni, S. Gimelli, M. Guipponi, M.F. Pelte, F. Bena, S.E. Antonarakis, A. Feki, Modelling and rescuing neurodevelopmental defect of Down syndrome using induced pluripotent stem cells from monozygotic twins discordant for trisomy 21, EMBO Mol. Med. 6 (2) (2014) 259–277.
[41] E.A. Markakis, F.H. Gage, Adult-generated neurons in the dentate gyrus send axonal projections to field CA3 and are surrounded by synaptic vesicles, J. Comp. Neurol. 406 (4) (1999) 449–460.
[42] K.C. Vadodaria, S. Jessberger, Functional neurogenesis in the adult hippocampus: then and now, Front. Neurosci. 8 (2014) 55.
[43] G. Kempermann, F.H. Gage, Genetic determinants of adult hippocampal neurogenesis correlate with acquisition, but not probe trial performance, in the water maze task, Eur. J. Neurosci. 16 (1) (2002) 129–136.
[44] P. Rakic, Adult neurogenesis in mammals: an identity crisis, J. Neurosci. 22 (3) (2002) 614–618.
[45] A. Alvarez-Buylla, J.M. Garcia-Verdugo, Neurogenesis in adult subventricular zone, J. Neurosci. 22 (3) (2002) 629–634.
[46] A. Ernst, K. Alkass, S. Bernard, M. Salehpour, S. Perl, J. Tisdale, G. Possnert, H. Druid, J. Frisen, Neurogenesis in the striatum of the adult human brain, Cell 156 (5) (2014) 1072–1083.
[47] E.H. Simpson, C. Kellendonk, E. Kandel, A possible role for the striatum in the pathogenesis of the cognitive symptoms of schizophrenia, Neuron 65 (5) (2010) 585–596.
[48] D. Inta, J.M. Lima-Ojeda, P. Gass, P. Fusar-Poli, Postnatal neurogenesis and dopamine alterations in early psychosis, Recent Pat. CNS Drug Discov. 7 (3) (2012) 236–242.
[49] X. Feng, K.A. Krogh, C.Y. Wu, Y.W. Lin, H.C. Tsai, S.A. Thayer, L.N. Wei, Receptor-interacting protein 140 attenuates endoplasmic reticulum stress in neurons and protects against cell death, Nat. Commun. 5 (2014) 4487.
[50] X. Feng, Y.L. Lin, L.N. Wei, Behavioral stress reduces RIP140 expression in astrocyte and increases brain lipid accumulation, Brain Behav. Immun. 46 (2015) 270–279.
[51] A. Izzo, R. Manco, F. Bonfiglio, G. Cali, T. De Cristofaro, S. Patergnani, R. Cicatiello, R. Scrima, M. Zannini, P. Pinton, A. Conti, L. Nitsch, NRIP1/RIP140 siRNA-mediated attenuation counteracts mitochondrial dysfunction in Down syndrome, Hum. Mol. Genet. 23 (16) (2014) 4406–4419.
[52] A. Izzo, N. Mollo, M. Nitti, S. Paladino, G. Cali, R. Genesio, F. Bonfiglio, R. Cicatiello, M. Barbato, V. Sarnataro, A. Conti, L. Nitsch, Mitochondrial dysfunction in down syndrome: molecular mechanisms and therapeutic targets, Mol. Med. 24 (1) (2018) 2.
[53] R.C. Scarpulla, Metabolic control of mitochondrial biogenesis through the PGC-1 family regulatory network, Biochim. Biophys. Acta 1813 (7) (2011) 1269–1278.